Article

Not peer-reviewed version

Diffusion Effect on Octogen Coating-Curing Kinetics with Polyurethane Using Infrared Spectroscopy

Heri Budi Wibowo *, Hamonangan Rekso Diputro Sitompul, Yudha Budiman, Bagus Wicaksono, Ahmad Jamaludin Fitroh, Ahmad Riyadl, Wiwiek Utami Dewi, Yulia Azatil Ismah, Dwi Setyaningsih, Aprilia Fitri Yastuti, Mohamad Baiquni, Lilis Mariani, Anggaria Maharani, Herry Purnomo, Kendra Hartaya, Retno Ardianingsih, Luthfia Hajar Abdillah, Sutrisno Sutrisno

Posted Date: 3 August 2023

doi: 10.20944/preprints202308.0226.v1

Keywords: polyurethane coating; kinetic; octogen, coating, curing, HTPB

Article

Diffusion Effect on Octogen Coating-Curing Kinetics with Polyurethane Using Infrared Spectroscopy

Heri Budi Wibowo [1]*, Hamonangan Rekso Diputro Sitompul [1], Yudha Budiman [1], Bagus Wicaksono [1], Ahmad Jamaludin Fitroh [1], Ahmad Riyadl [1], Wiwiek Utami Dewi [1], Yulia Azatil Ismah [1], Dwi Setyaningsih [1], Aprilia Fitri Yastuti [1], Mohamad Baiquni [2], Lilis Mariani [1], Anggaria Maharani [3], Herry Purnomo [1] , Kendra Hartaya [1], Retno Ardianingsih [1], Luthfia Hajar Abdillah [1] and Sutrisno [1]

[1] Aeronautics and Space Research Organization, National Research and Innovation Agency, Cibinong, 16911, West Java, Indonesia; hamo001@brin.go.id (H.R.D.S); yudh002@brin.go.id (Y.B.); bagu005@brin.go.id (B.W.); ahma056@brin.go.id (A.J.F.); ahma052@brin.go.id (A.R.); wiwi015@brin.go.id (W.U.D.); yuli042@brin.go.id (Y.A.I.); dwis011@brin.go.id (D.S.); apri012@brin.go.id (A.F.Y.); lili007@brin.go.id (L.M.); herr010@brin.go.id (H.P.); kend001@brin.go.id (K.H.); retn014@brin.go.id (R.A.); luth002@brin.go.id (L.H.A.); sutr004@brin.go.id (S).

[2] Directorate of Laboratory Management, Research Facilities, and Science and Technology Area, Deputy for Research and Innovation Infrastructure, National Research and Innovation Agency, Central Jakarta, Jakarta, 10340, Indonesia; moha040@brin.go.id

[3] Energetic Material Center, DAHANA Co., Subang, West Java, 41285, Indonesia; angaria.maharani@dahana.id

* Correspondence: heribw@gmail.com; Tel.: +62-021-4892802

Abstract: The kinetic analysis of octogen coating with a polyurethane base containing hydroxyl-terminated polybutadiene (HTPB) was investigated using infrared spectroscopy. The coating process involved a solvent method, where octogen and liquid polyurethane were mixed, the solvent was evaporated, and curing took place at an elevated temperature. The ratio of HTPB to diisocyanate was equimolar. Initially, the curing process occurred in the solvent system, followed by further curing in the bulk system. The kinetic analysis was performed using a modified diffusion-autocatalytic model, which includes non-catalytic, autocatalytic, and diffusion components. This model was compared with others during the bulk reaction and proved to be effective in correcting errors, particularly in the gel time region. Thermodynamic parameters were evaluated using the Arrhenius and Eyring equations. The reaction rate was initially controlled by chemical reactivity, but after the gel time, diffusion became the controlling factor. In the HTPB-TDI system, both the non-catalytic and autocatalytic parts decreased with increasing temperature, while diffusivity increased. It is worth noting that diffusivity is temperature-dependent. Different diisocyanates, namely toluene diisocyanate (TDI), isophorone diisocyanate (IPDI), and hexamethylene diisocyanate (HMDI), were studied, revealing that HMDI exhibited higher reactivity than TDI and IPDI. The catalyst effect on reaction rate HTPB-TDI system is investigated. Catalysts adding (0.1%) to HTPB-TDI system is really decrease their activation energy by efectivity DBTL>FeAA>TPB. Catalyst not change their diffusivity.

Keywords: polyurethane coating; kinetic; octogen; coating; curing; HTPB

1. Introduction

Hexogen and octogen are both high explosive materials. They are used as oxidants in homogeneous propellants due to their high energy content, substituting ammonium perchlorate in composite propellant formulations (APCP) [1–3]. The addition of coated hexogen to the composite propellant formulation can increase its energetic properties and reduce smoke emissions. However, these explosives have disadvantages as they are sensitive and not compatible with the HTPB (Hydroxyl Terminated Polybutadiene) binder, necessitating a coating process [3–11].

Hexogen powder has been successfully coated using polyurethane-based HTPB through a solvent method. In this process, the powder is mixed with the coating solution, and polymerization

 doi:10.20944/preprints202308.0226.v1

is initiated within the solution. Subsequently, the solvent is evaporated, and the polyurethane coating is cured at an elevated temperature. There is limited research information about explosive coating kinetics; most publications focus on characterizing the coated hexogen and their propellant properties.

Additional research is needed to further investigate and understand the coating kinetics of octogen with polyurethane-based HTPB, as well as the potential for using different catalysts and diisocyanates in the coating process. Catalysts play a significant role in accelerating the reaction rate during polymerization. Some suitable catalysts for polyurethane include tri ethylene diamine (TEDA), dibutyl tin laurate (DBTL), tin (II) 2-ethyl hexanoate, and tris phosphine bismuth (TPB). Additionally, there are several diisocyanates that can be used as curing agents, such as toluene diisocyanate (TDI), isophorone diisocyanate (IPDI), phenyl diisocyanate (PDI), and hexamethylene diisocyanate (HMDI). This paper focuses on the kinetic approach of coating octogen with polyurethane-based HTPB using varied diisocyanates (TDI, IPDI, and HMDI) and the most commonly used catalysts (TPB, FeAA, and DBTL) [3,5,7,14].

Polyurethane curing kinetics have been extensively studied using various methods such as infrared spectroscopy, NMR, viscosity, and heat release measurements [12–16]. Among these, infrared spectroscopy stands out as the simplest, most accurate, rapid, and cost-effective method for evaluating this kinetic model. The reaction conversion is assessed by observing the absorption of isocyanate groups, with polybutadiene methyl groups used as an absorption reference. Quantitative analysis is then performed using a calibration curve. The coating and infrared characterization of hexogen are successfully achieved using polyurethane and Viton [1,2].

The kinetic of bulk polyurethane formation has been investigated intensively. Kinetic models for polyurethane formation can be broadly classified into non-catalytic and autocatalytic models. The non-catalytic model is based on the linear formation of polyurethane between alcohol (HTPB) and diisocyanate, but it is only suitable for low viscosity conditions before gel time. On the other hand, the autocatalytic model involves the addition of crosslinks in polyurethane formation between urethane and excess diisocyanate. This model dominates at elevated temperatures or when excess diisocyanate is present and is more appropriate for gel time to high viscosity scenarios. However, this model is not suitable for the curing process of undeformed cured polyurethane, as the curing in such cases is controlled by molecular diffusivity. To address this, the modified autocatalytic model has been developed, taking diffusion effects into account.

In the powder coating process using the solvent method, the curing occurs through two reaction stages. Initially, the curing reaction is initiated in the solution phase during the mixing of HTPB, diisocyanate, and substrate. At this stage, the reactant molecules exhibit high activity, allowing for easy migration and collision, and the reaction is primarily controlled by their chemical reactivity. As the reaction progresses, after the gel time, the second stage of curing takes place in a solid coating film formed when all solvents evaporate [1,3–8]. During this stage, the activity of the reactant molecules is hindered by their diffusivity in the film. The reactivity of system isopropyl diol and phenyl diisocyanate is controlled by their diffusivity in the film state at high temperature and high viscosity [8].

In the first stage of curing, the reactants display high activity, and the reaction is mainly governed by their chemical reactivity. However, after the evaporation of solvents, the reaction rate is then controlled by film diffusion. For the coating system involving isopropyl di-alcohol and methylene diisocyanate, the first curing stage is governed by chemical reactivity, while the subsequent curing stage is controlled by intra-film diffusion at higher temperatures [17]. Therefore, investigating the diffusivity effect on the kinetic process during the coating is essential.

The kinetics of octogen and hexogen coating with polyurethane-based HTPB are studied using infrared spectroscopy with varied diisocyanates and catalysts. The diffusion effect on the reaction rate and thermodynamic parameters, such as activation energy, enthalpy, and entropy, is studied using the modified autocatalytic model. Additionally, the temperature effect on the reaction is determined using the Arrhenius and Eyring equations.

Preprints (www.preprints.org) | NOT PEER-REVIEWED | Posted: 3 August 2023 doi:10.20944/preprints202308.0226.v1

2. Materials and Methods

2.1. Materials

Octogen was supplied by DAHANA, Co., Ltd. Ethyl acetate for pure analysis was supplied by Merck. HTPB, IPDI, TDI, HMDI, DBTL, TPB, and FeAA were supplied by Dalian, Co., Ltd. The HTPB has a hydroxyl number of 40, functionality of 1.9, average molecular weight of 3000 g/mol, and polydispersity index of 1.3. The particle size of the octogen was 100 microns.

2.2. Instrumentations

Infrared qualitative and quantitative analysis was conducted using a Hitachi IR-Prestige Serial A210043 infrared spectrometer with a standard liquid cuvette, covering the wavelength range of 400-4000 cm^{-1} [9–11]. The coating depth was measured using a Scanning Electron Microscope (SEM) Phenom Word Pro X Desktop [8,9,12]. The particle size of the octogen was measured with a particle size analyzer PSA-1232.

2.3. Procedure

A mixture of 4 mL of HTPB, 50 mL of ethyl acetate, 0.4 mL of TDI, and 200g of octogen is prepared in a 500 mL glass beaker and stirred for 60 minutes [13,14]. The molar ratio of isocyanate to hydroxyl is maintained as equimolar (R=1). Approximately 1 mL of the mixture is withdrawn as a sample every 5 minutes, dissolved in 100 mL of benzene, and analyzed using infrared spectroscopy [19–21]. The filtrated ethyl acetate is then evaporated and the residue is dried in a vacuum oven for 15 minutes at 40°C. The resulting film-coated octogen is casted into a KBr pellet and cured in the oven for 7 days at 40°C. The cured and coated octogen is subjected to infrared analysis every hour during the curing process. After curing, the shape of the coated octogen particles is analyzed using SEM [26,40,41]. This procedure is repeated for temperature curing 50, 60, 70°C.

The above procedure is repeated using different diisocyanates, namely IPDI and HMI. Additionally, the effect of catalysts is studied by adding 0.1g of FeAA, DBTL, and TPB as catalysts.

2.4. Analysis

The reaction conversion is determined by measuring the change in isocyanate concentration, which is identified through infrared absorption of the isocyanate stretching vibration in the isocyanate group, occurring at 2250-2275 cm^{-1}. To establish a constant reference, the absorption of CH3 vibration in the polybutadiene (HTPB) at 2850-2950 cm^{-1} is used. The reaction conversion (α) is calculated using Eq-1, where A^{o}_{NCO} and A^{o}_{CH3} represent the initial absorbance of NCO and CH3 absorption, respectively.

$$\propto = 1 - \frac{A_{NCO}/A_{CH3}}{A^{o}_{NCO}/A^{o}_{CH3}} \quad (1)$$

2.5. Kinetics Model

The kinetic model for polyurethane formation from HTPB and diisocyanate is based on the reaction of hydroxyl groups from HTPB with isocyanate from diisocyanate, resulting in the production of urethane groups, as shown in Eq-2. The mechanism of this reaction is complex [7,18–20].]. The polymerization process involves the addition of chains of urethane, and the kinetic model is based on the reaction of functional groups, showing a reaction of n-order, as expressed in Eq-3. This model is referred to as the non-catalytic model and effectively predicts the formation of polyurethane at low polymer chain lengths or before the gel time.

$$\text{-N=C=O + HO-} \rightarrow \text{-NH-CO-O-} \quad (2)$$

$$\frac{d\propto}{dt} = k(1-\propto)^{n} \quad (3)$$

Preprints (www.preprints.org) | NOT PEER-REVIEWED | Posted: 3 August 2023 doi:10.20944/preprints202308.0226.v1

The non-catalytic model struggles to accurately predict the reaction rate profile for higher polymer chains after the gel phase. To address this limitation, the model incorporates an autocatalytic reaction between urethane and isocyanate, leading to the production of crosslink allophanate as described in Eq-4. This autocatalytic reaction becomes more prominent at higher temperatures when there is an excess of isocyanate. The model incorporates two reaction rates: k_1 for linear polymerization contribution and k_2 for crosslink contribution, expressed in Eq-5. The crosslink reaction follows an m-order reaction.

-N=C=O + -NH-CO-O-→ -N-(CO-O-)(CO-NH-) (4)

$$\frac{d\propto}{dt} = (k_1 + k_2 \propto^m)(1-\propto)^n \quad (5)$$

This polyurethane formation is well predicted, but deviations increase at higher temperatures. The model is controlled by chemical reaction kinetics, and the diffusion is negligible. The diffusion's contribution to polyurethane curing is proposed to be related to the crosslink reaction and is expressed in Eq-6, where D represents diffusivity. D and m are affected by the reaction temperature.

$$\frac{d\propto}{dt} = k_1(1-\propto)^n + \frac{k_2 \propto^m (1-\propto)^n}{1+(\propto/_D)} \quad (6)$$

The thermodynamic parameters are evaluated using the Arrhenius and Eyring relations, which are expressed in Eq-7 and Eq-8 [12,38,39]. In these equations, the symbols A_k, E, A, R, T, N, h, ΔS, and ΔH represent the reaction rate constant, activation energy, collision frequency, enthalpy, and entropy of the i-th reaction. Additionally, A, R, T, h, and N represent the ideal gas constant (8.314 $J.mol^{-1}.K^{-1}$), reaction temperature (K), Planck constant ($6.626x10^{-34}$ J.s.), and Avogadro number ($6.022x10^{\wedge 23}$ mol^{-1}).

$$ln\ k_i = -\frac{E_i}{RT} + \ln A_i \quad (7)$$

$$\ln\left(k_i/_T\right) = -\frac{\Delta H_i}{RT} + \frac{\Delta S_i}{RT} + \ln\frac{R}{Nh} \quad (8)$$

3. Results and Discussion

3.1. Coating identification

The particle size analysis reveals a significant increase in the size of octogen particles, from 100 to 200 microns. Figure 1 shows the SEM image of the particles. The circularity and roundness of the particles are calculated using Image-J software, and it is observed that the circularity has increased from 0.74 to 0.76, while the roundness has increased from 0.67 to 0.72. The presence of mounds, as indicated by arrows, signifies the presence of a polyurethane layer coating on the octogen particles. Based on the image and particle size analysis, it can be concluded that octogen has been well coated with polyurethane-based HTPB. These results align with the findings of Wibowo et al.. [7,19,23,24], who studied the coating of hexogen with HTPB-based polyurethane.

Preprints (www.preprints.org) | NOT PEER-REVIEWED | Posted: 3 August 2023 doi:10.20944/preprints202308.0226.v1

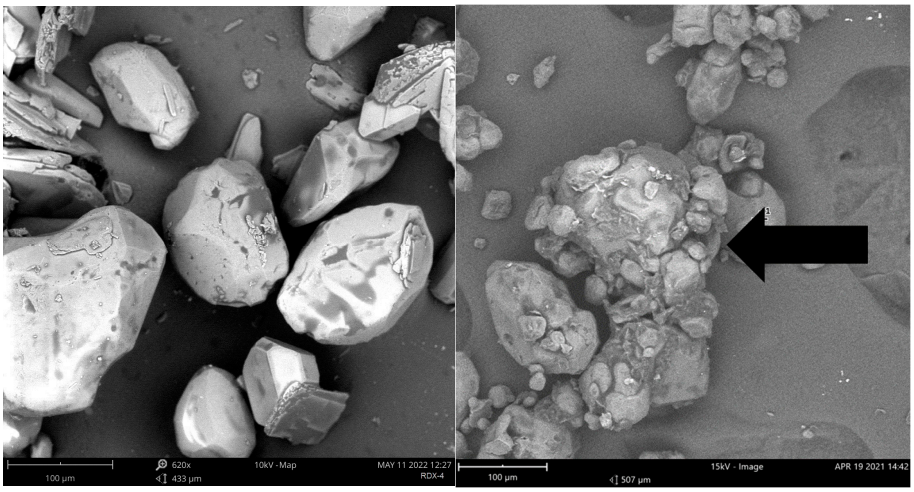

(a) (b)

Figure 1. SEM analysis of octogen (a) and coated octogen (b).

3.2. IR identification

Figure 3 displays the infrared spectra of coated octogen in both the slurry (a) and film state (b). The octogen is identified by its characteristic absorption bands, including nitro groups at 1566 cm^{-1} (νs NO_2), 1142 cm^{-1} (ν ring), 964 and 949 cm^{-1} (stretching bands), 833 and 764 cm^{-1} (δ and γ NO_2), and 625 and 602 cm^{-1} (T+γ NO_2) [1,2,7,19] . These characteristic absorption bands are also observed in the spectra of coated octogen

The polyurethane is produced through a reaction between isocyanate and alcohol [3]. The isocyanate group induces the formation of electrophilic centers at nitrogen atoms and nucleophilic centers at oxygen atoms. Nucleophiles containing active hydrogen from HTPB can attack the isocyanate, resulting in the acceptance of hydrogen atoms by oxygen atoms to produce unstable carbonyl groups. After molecular rearrangement, the urethane NCOO groups are formed. This reaction can be identified by a decrease in the isocyanate group's absorption at wavelengths of 2260-2275 cm-1. The polyurethane formation is indicated by an increase in the absorption of C=O stretching at 1600-1750 cm^{-1} and NH stretching at 1500-1550 cm^{-1} [26,27].

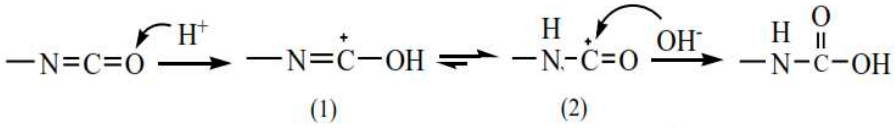

The backbone of HTPB is identified by the absorption of CH_2 stretching and CH_3 at 1640 and 2850-2950 cm^{-1}, respectively. This absorption remains unchanged throughout the reaction. The decrease in isocyanate concentration is identified by the reduction of NCO absorption at 2270 cm^{-1} [1]. At the end of the reaction, there is no absorption of NCO at 2270 cm-1, indicating that all of the isocyanate has reacted. HTPB is further identified by the absorption of C=C stretching and CH3 stretching at 1640 and 2850-2950 cm-1, respectively. This absorption remains unchanged throughout the reaction, making it suitable as a reference. The formation of polyurethane can be identified by the absorption of C=O stretching vibration at 1710-1760 cm^{-1}.

Preprints (www.preprints.org) | NOT PEER-REVIEWED | Posted: 3 August 2023 doi:10.20944/preprints202308.0226.v1

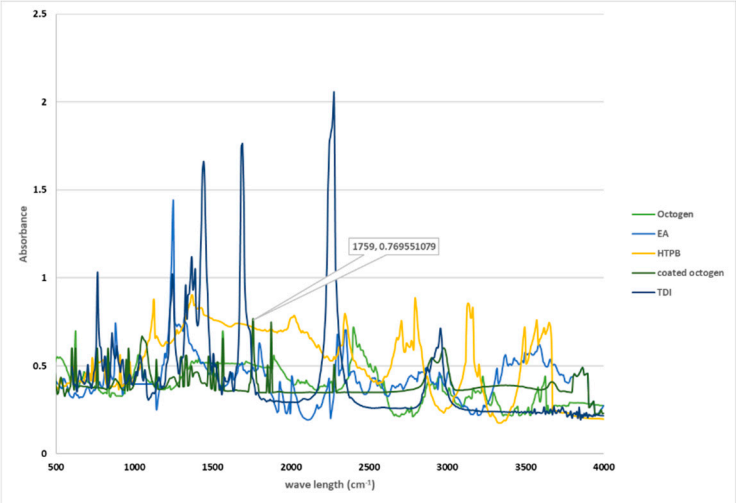

Figure 2. The infrared spectra of coated octogen.

3.3. Kinetic Evaluation

The modified diffusion-autocatalytic model is applied to the HTPB-TDI system using Eq-6. The experimental data is fitted to plot log(dα/dt) versus (1-α) in Figure 2. The values of 'n' and 'k1' are determined from their slope and intercept. The parameters k2, m, and D are repeated for temperatures 40, 50, 60, and 70°C, and the kinetic parameter values are summarized in Table 1.

The calculated kinetic parameters are compared to the non-catalytic model (Eq-2) and the autocatalytic model equation (Eq-4). The fit of calculated cure conversion to the experimental data of the varied model is shown in Figure 3. The modified diffusion-autocatalytic model exhibits a lower error (R=0.9987) compared to the other models (R=0.9953 and 0.9978). Non-catalytic models tend to yield higher estimates of experimental results than autocatalytic models. The autocatalytic model incorporates an allophane formation reaction as shown in Eq-3. Crosslinks begin to appear when a considerable amount of urethane group is formed, primarily near the gel time [28]. A competitive reaction occurs between urethane and allophanate formation, leading to different reaction rates in the gel time regions. The role of diffusivity becomes evident from the beginning of the gel time to the end of the reaction. The autocatalytic model is improved by adding a diffusion component, which brings the calculated curing conversion closer to the experimental results. Similar results were observed when applying the diffusion model to HTPB-IPDI with high solid content [29]. These results also apply to cases without filler and low concentration, where the diffusion effect significantly corrects the error across the entire reaction range. The influences of chemical reactivity (electronegativity and steric hindrance), crosslink reactions (allophanate formation), and molecule diffusivity have been incorporated into the non-catalytic, autocatalytic, and diffusion parts, respectively.

The reaction initially occurs in solution with low viscosity, where the movement of molecules is not affected by diffusion [[29]. The reaction initially occurs in solution with low viscosity, where the movement of molecules is not affected by diffusion [[29]. This is because the reaction is carried out without solvents or at high concentrations, allowing diffusivity to take effect at the beginning of the reaction. As the gel time approaches, the profile starts to deviate lower than the experimental data because some urethane groups react with the isocyanate to form allophanate. Both the autocatalytic part and diffusivity significantly contribute to the curing conversion, and all parts significantly contribute to the reaction rate. After the gel time, the diffusivity part becomes dominant in contributing to the reaction rate, as seen by the increasing total rate constant every ten degrees temperature. With every ten-degree increase in temperature, the total constant rate increases by 1.1 (less than 1.2), indicating that diffusion controls the reaction rate.

Preprints (www.preprints.org) | NOT PEER-REVIEWED | Posted: 3 August 2023 doi:10.20944/preprints202308.0226.v1

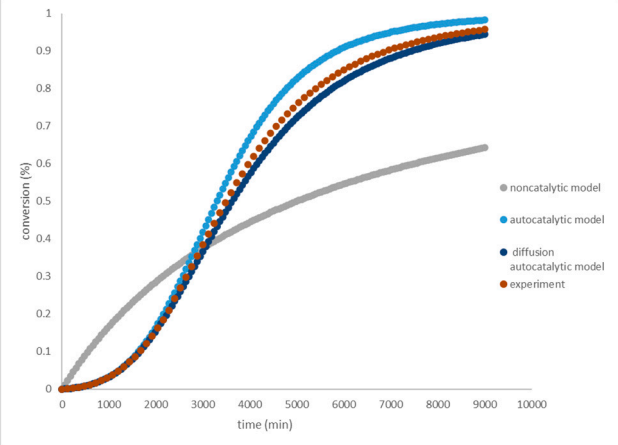

Figure 2. Plotting curing conversion of HTPB-TDI system at variated model.

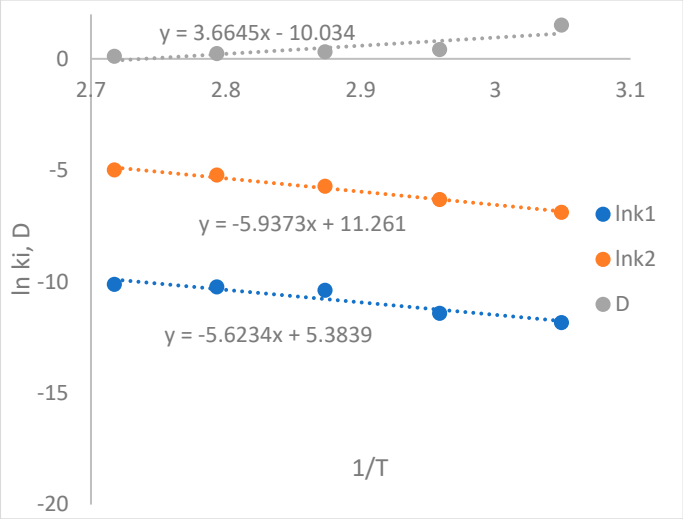

Figure 3. plotting ln k and D versus 1/T.

At a temperature of 30°C, the catalytic rate (k1) is generally lower than the autocatalytic rate (k2). This phenomenon is commonly observed in polyurethane systems, similar to HTPB-IPDI [29]. Based on the reaction mechanisms described in Eq-1 and Eq-3, the isocyanate group is more susceptible to attack by nucleophilic H+ from hydroxylated HTPB than from urethane [31]. This observation is supported by infrared spectrometer results, which consistently show the presence of the urethane group (indicated by C=O stretching vibration absorption) along with the appearance of the allophanate group.

Table 1. The calculate k_1, m, k_2 and D of HTPB-TDI system at variated temperature.

Temperature (oC)	k_1 (s^{-1})	n	k_2 (s^{-1})	D	m
30	$8.10x10^5$	1.2	$1.01x10^4$	1.51	0.8
40	$14.10x10^5$	1.2	$1.43x10^4$	0.41	0.8
50	$21.10x10^5$	1.2	$1.71x10^4$	0.31	0.8
60	$26.10x10^5$	1.2	$2.01x10^4$	0.23	0.8
70	$31.10x10^5$	1.2	$2.57x10^4$	0.11	0.8

The temperature-raising effect in Figure 2 shows that both k1 and k2 increase, while D decreases. This phenomenon aligns with the behavior observed in the diffusivity of the HTPB-IPDI system, where diffusivity increases as a function of viscosity [32]. The thermodynamic parameters are

Preprints (www.preprints.org) | NOT PEER-REVIEWED | Posted: 3 August 2023 doi:10.20944/preprints202308.0226.v1

calculated using the Arrhenius and Eyring equations and are summarized in Table 2. The relationship between ln(k_1), ln(k_2), and (1/T) is illustrated in Figure 4. Similarly, the relation of D versus (1/T) is plotted in Figure 5. The calculated activation energy of the non-catalytic part (Ea_1) and autocatalytic part (Ea_2) are 35 and 39 kJ/mol, respectively. The relationship between diffusion and temperature is described by the equation -54.33 + 31,541/T. The activation enthalpy and entropy of curing are obtained from plotting ln(k/T) versus (1/T), as shown in Figure 6. The values of ΔS and ΔH are summarized in Table 2. It is observed that the activation entropy of k_1 is negatively larger than k_2, indicating that the catalytic part exhibits easier formation of the transition state.

Table 2. The thermodynamic parameter of HTPB-TDI system.

part	E_a (kJ·mol^{-1})	A (L.mol^{-1}·min^{-1})	ΔH (kJ·mol^{-1})	ΔS (J·mol^{-1}·K^{-1})
Non-catalytic (k_1)	39	11.732	33	-198
Autocatalytic (k_2)	47	31,037	41	-148

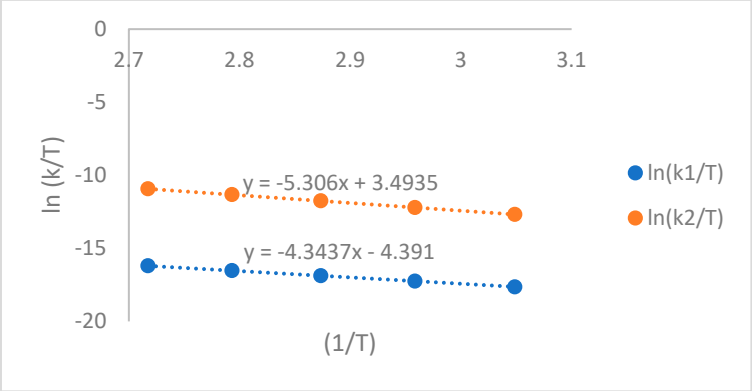

Figure 4. Plotting ln(k/T) versus (1/T).

Based on the calculated thermodynamic parameter, the reaction rate equation of HTPB-TDI is modeled by Eq-10.

$$\frac{d\alpha}{dt} = \left[\left[11.7exp\left(-\frac{35000}{RT}\right) * (1-\alpha)^{1.2}\right]\right] + \frac{\left[\left[31{,}077exp\left(-\frac{47000}{RT}\right) * \alpha^{0.8} * (1-\alpha)^{1.2}\right]\right]}{\left[1+\left(\alpha/(45+2754/T)\right)\right]} \quad (10)$$

3.4. Diisocyanate effect

The plot of curing conversion at 30°C is shown in Figure 4. The average fitting correlation (R2) is greater than 0.9980, indicating that this model accurately predicts the reaction rate. The predictions made by this model are more precise than both the non-catalytic and autocatalytic models used in the HTPB-IPDI system.

Preprints (www.preprints.org) | NOT PEER-REVIEWED | Posted: 3 August 2023 doi:10.20944/preprints202308.0226.v1

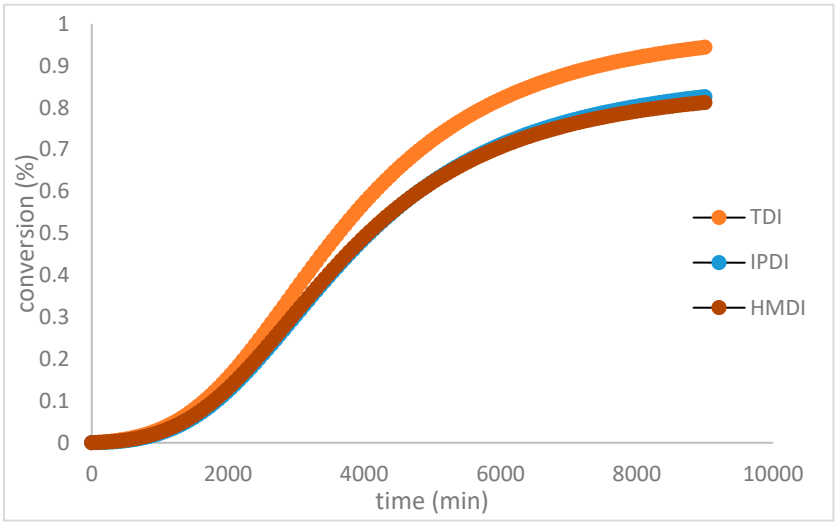

Figure 4. The curing conversion profile of polyurethane based HTPB at variated diisocyanate.

The kinetic parameters of polyurethane-based HTPB with various diisocyanates have been evaluated and summarized in Table 3. The effect of diisocyanate type on the reaction rate is evident from their respective activation energies. The reactivity of isocyanate follows the order: HMDI >TDI> IPDI, with activation energies of 35, 39, and 45 kJ/mol, respectively. Both the non-catalytic and autocatalytic parts show a similar trend in this regard. For the HTPB-IPDI system, the values of Ea1 and Ea2 are comparable to those of the autocatalytic model, with values of 45.12 and 54.12 kJ/mol [31]. The faster reactivity of HMDI compared to TDI can be attributed to their structural differences. The aliphatic nature of MDI results in less electron shifting towards the isocyanate group compared to the aromatic system of TDI, leading to a more negatively charged isocyanate, as observed in Figure 5. A similar reactivity pattern has been observed in experiments involving saturated polyester with HMDI and phenyl diisocyanate [33]. The reactivity of isocyanates is influenced by the positive nature of the carbon atom, which acts as a nucleophilic center.

Table 3. The kinetic parameters of polyurethane based HTPB at variated isocyanate.

System	E_{a1} (kJ·mol^{-1})	E_{a2} (kJ·mol^{-1})	D=A+B/T
HTPB-TDI	37	47	-54.33+31,541/T
HTPB-IPDI	34	52	-35.12+21,227/T
HTPB-HMDI	59	49	-72.09+37,001/T

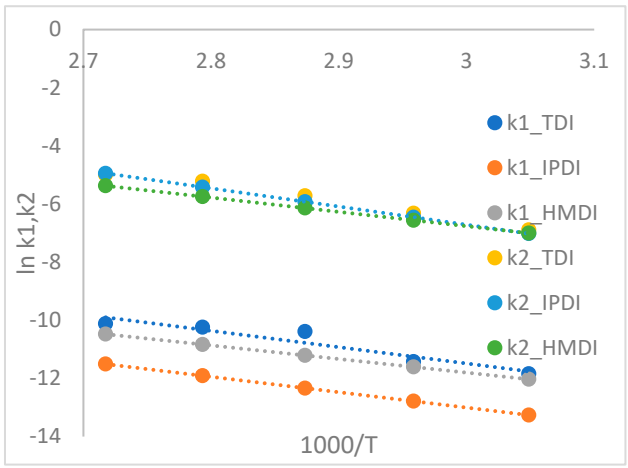

Preprints (www.preprints.org) | NOT PEER-REVIEWED | Posted: 3 August 2023 doi:10.20944/preprints202308.0226.v1

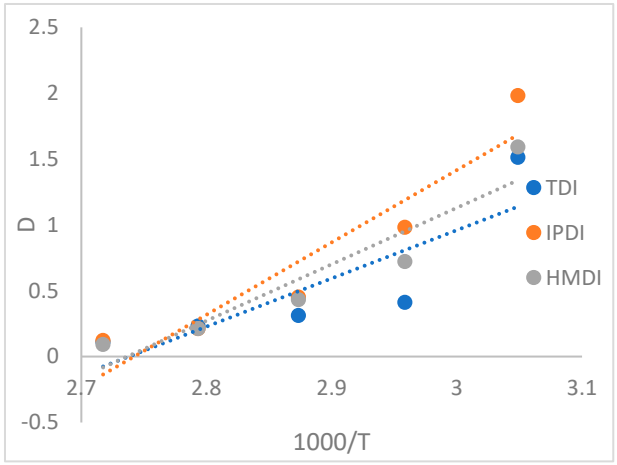

Figure 5. Plotting ln(k) and D versus (1/T).

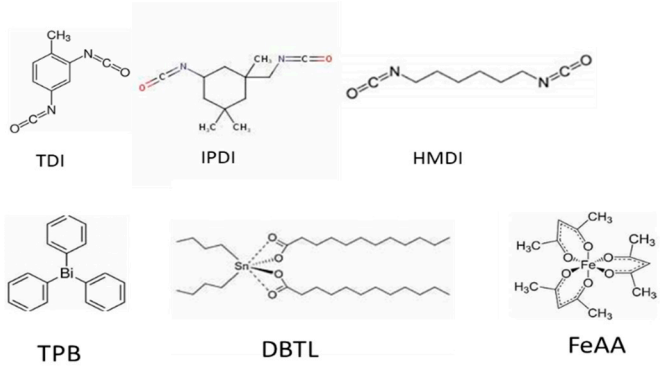

Figure 6. structure of diisocyanate and catalyst.

The effect of diffusivity on the reaction rate is observed in Table 3, where the diffusion part constant (B) represents this impact. The calculated B value for the HTPB-IPDI system is similar to that observed in a previous experiment with a high filled state [32]. The diffusion effect is most significant in the following order: HTPB-HMDI > HTPB-TDI > HTPB-IPDI. It is important to note that the diffusion effect differs from the effect on the reaction rate and is primarily influenced by the movement of molecules. This diffusivity is directly related to the solubility of the substances, and the solubility can be predicted using group contribution methods [32]. The calculated solubility values for HTPB, HMDI, TDI, and IPDI are 0.12, 12.03, 17.01, and 25.02 g/L, respectively. Among these, HTPB-HMDI has the lowest solubility, followed by HTPB-TDI and HTPB-IPDI. The solubility of HMDI is lower than that The diffusivity is directly related to the solubility of the substances, and the solubility can be predicted using group contribution methods of IPDI and TDI.

3.5. Catalyst addition

The effect of catalysts on the HTPB-TDI system is studied using triphenyl bismuth (TPB), ferrous tris-acetylacetonate (FeAA), dibutyl tin laurate (DBTL), and TECH. TPB and DBTL are commonly used as curing catalysts for composite propellants based on HTPB. The curing conversion profiles of HTPB-TDI with various catalysts are illustrated in Figure 7. All the added catalysts result in a higher slope compared to the system without any catalyst.

Preprints (www.preprints.org) | NOT PEER-REVIEWED | Posted: 3 August 2023 doi:10.20944/preprints202308.0226.v1

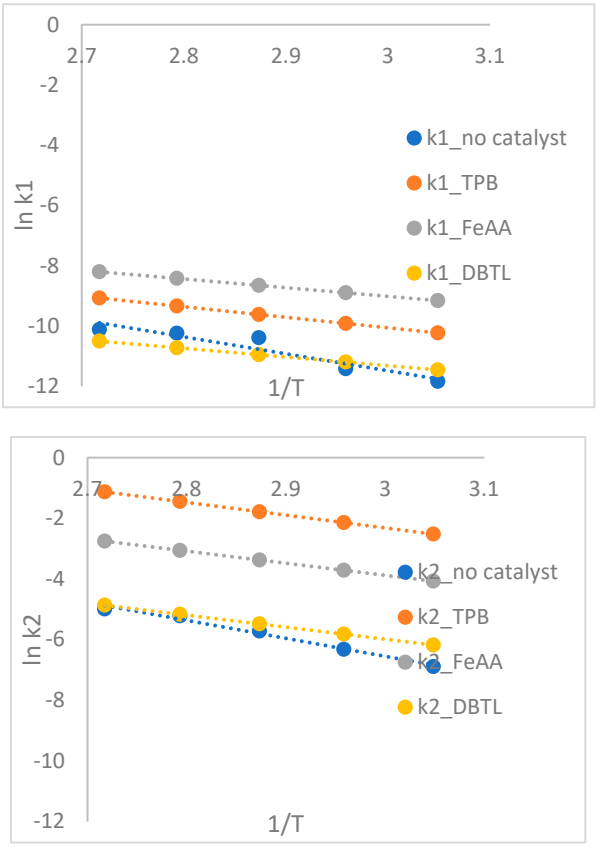

Figure 7. Plotting ln k1 and k2 to (1/T).

The effect of adding catalysts on the activation energy and diffusivity of the curing process is summarized in table 4. The activation energy decreases with the addition of catalysts: from 35 to 29 kJ.mol^{-1} for TPB, 24 kJ.mol^{-1} for FeAA, 19 kJ.mol^{-1} for DBTL, and 21 kJ.mol^{-1} for TECH. The effectiveness of the catalysts in enhancing the reaction rate follows the order: DBTL > TPB > FeAA. These results are consistent with previous experiments involving the addition of DBTL catalyst to HTPB-IPDI using the non-catalytic model. In those experiments, DBTL was found to decrease the activation energy from 41 to 38 kJ.mol^{-1}, 28 to 17 kJ.mol^{-1} for stearate-terminated hyperbranched polyether, and 35 to 31 kJ.mol^{-1} for TECH [26,35–37]. The addition of DBTL and TECH catalysts also decreased the gel time from 200 minutes to 16 minutes and 114 minutes, respectively [26]. The diffusivity also decreased with the addition of catalysts, following the same trend as the activation energy: DBTL > TPB > FeAA > TECH. This suggests that both reactivity and diffusivity are affected similarly by the addition of catalysts [17,38,39].

Table 4. Calculated solubility index of diisocyanate.

System	Calculated Solubility (J/cm^3)$^{1/2}$
HTPB	17.6
TDI	13.8
IPDI	12.01
HMDI	16.51
TPB	18.12
FeAA	15.35
DBTL	20.38
Ethyl acetate	20.8

Preprints (www.preprints.org) | NOT PEER-REVIEWED | Posted: 3 August 2023 doi:10.20944/preprints202308.0226.v1

Table 5. The kinetic parameters of HTPB-TDI system with variated catalyst.

System	E_{a1} (kJ·mol^{-1})	E_{a2} (kJ·mol^{-1})	D=A+B/T
HTPB-TDI no catalyst	35	39	-54.33+31,541/T
HTPB-TDI-TPB	29	35	-54.23+27,412/T
HTPB-TDI-FeAA	24	33	-53.09+25,114/T
HTPB-TDI-DBTL	19	25	-54.12+28,211/T

The phenomenon can be explained by the relationship between reactivity and the solubility of each catalyst [17,38,39]. Catalysts are added to accelerate the urethane formation, and polar interactions between hydroxyl or isocyanate and the catalyst occur, enhancing the electrophilic character of the carbon of the NCO groups [34] . Organotin catalysts, such as DBTL, follow a Lewis-acid mechanism, as illustrated in Fig-3. Tin carboxylate bonds are hydroxylated to produce active intermediates, which then undergo nucleophilic attack by alcohol and the original C=O to form Sn complexation. Isocyanate is activated by coordination to the active Sn-OR intermediate via oxygen or nitrogen, followed by the nucleophilic attack of the hydroxyl group from the alcohol

The structure of the catalyst is illustrated in Figure 7, and it can be simplified into core and shell parts, with the core being rich in OH groups that are ready to form hydrogen bonds with NCO groups. The solubility parameters of TDI and HTPB are 13.8 and 17.6 $(J/cm^{-3})^{1/2}$, respectively, while the solubility parameters of DBTL, TPB, FeAA, and TECH are 20.38, 18.12, 15.35, and 12.77 $(J/cm^{-3})^{1/2}$. The higher solubility of the catalysts contributes to their OH-rich character, which enhances their bonding with isocyanate. Higher solubility also increases their diffusivity.

4. Conclusions

The infrared spectroscopy was used to conduct a kinetic analysis of octogen coating with a polyurethane base containing hydroxyl-terminated polybutadiene (HTPB). The coating process involved a solvent method where octogen and liquid polyurethane were mixed, followed by solvent evaporation and curing at an elevated temperature. The curing process initially occurred in the solvent system and continued in the bulk system.

The kinetic analysis was performed using a modified diffusion-autocatalytic model, which includes non-catalytic, autocatalytic, and diffusion components. This model was effective in correcting errors observed in other models, particularly in the gel time region. The reaction rate was primarily controlled by chemical reactivity initially, but after the gel time, diffusion played a significant role. The diffusivity was influenced by temperature variations.

The reaction rate of diisocyanates followed the sequence HMDI > TDI > IPDI due to their chemical structure. However, the effect of diffusivity increased in the sequence IPDI > HMDI > TDI, influenced by their solubility. When catalysts were added to the HTPB-TDI system, they significantly contributed to reducing the activation energy. The catalysts TPB, FeAA, and DBTL decreased the activation energy in the order DBTL>FeAA>TPB.

Author Contributions: Conceptualization, Heri Budi Wibowo and Hamonangan Rekso Diputro Sitompul; Data curation, Heri Budi Wibowo, Hamonangan Rekso Diputro Sitompul, Ahmad Jamaludin Fitroh, Dwi Setyaningsih, Aprilia Fitri Yastuti and Mohamad Baiquni; Formal analysis, Heri Budi Wibowo and Hamonangan Rekso Diputro Sitompul; Funding acquisition, Heri Budi Wibowo; Investigation, Heri Budi Wibowo, Hamonangan Rekso Diputro Sitompul, Yudha Budiman, Wiwiek Utami Dewi, Yulia Azatil Ismah, Retno Ardianingsih and Luthfia Hajar Abdillah; Methodology, Heri Budi Wibowo, Hamonangan Rekso Diputro Sitompul and Kendra Hartaya; Project administration, Heri Budi Wibowo and Anggaria Maharani; Resources, Heri Budi Wibowo; Software, Heri Budi Wibowo, Hamonangan Rekso Diputro Sitompul, Ahmad Jamaludin Fitroh, Ahmad Riyadl and Herry Purnomo; Supervision, Heri Budi Wibowo; Validation, Heri Budi Wibowo, Hamonangan Rekso Diputro Sitompul, Bagus Wicaksono and Sutrisno; Visualization, Heri Budi Wibowo; Writing – original draft, Heri Budi Wibowo; Writing – review & editing, Heri Budi Wibowo, Hamonangan Rekso Diputro Sitompul Sutrisno and Lilis Mariani. All authors have read and agreed to the published version of the manuscript."

Funding: The Authors would like to express their gratitude to Rispro-LPDP Fund Program Batch-II, through Competitive Research RISPRO-LPDP Program for financial support in doing this research with contract No. 082.01.06.3534.001.002.053A.524119 and Skep-27/LPDP/2020.

Institutional Review Board Statement: Not applicable.

Informed Consent Statement: Not applicable.

Data Availability Statement: The data presented in this study are available on request from the corresponding author.

Acknowledgements: The authors would like to convey our gratitude towards Rocket Technology Center and Dahana Co.Ltd.

Conflicts of Interest: The authors declare no conflict of interest.

References

1. H. Wibowo *et al.*, "Hexogen Coating Kinetics with Polyurethane-Based Hydroxyl-Terminated Polybutadiene (HTPB) Using Infrared Spectroscopy," *Polymers (Basel)*, vol. 14, p. 1184, Jul. 2022, doi: 10.3390/polym14061184.
2. E. da Costa Mattos *et al.*, "Characterization of Polymer-Coated RDX and HMX Particles," *Propellants, Explosives, Pyrotechnics*, vol. 33, no. 1, pp. 44–50, Feb. 2008, doi: 10.1002/prep.200800207.
3. Y. Yano and T. Gomi, "Burning rate characteristics of RDX-CMDB propellants.," *Journal of the Japan Society for Aeronautical and Space Sciences*, vol. 34, no. 391, pp. 447–452, 1986, doi: 10.2322/jjsass1969.34.447.
4. H. B. Wibowo and R. S. M. Wibowo, "Non Energetic Binder Application for RDBP Propellant Based Large Caliber Munition (MKB)," *International Seminar on Aerospace Science and Technology IV*, pp. 82–91, 2016.
5. S. Lee, I.-K. Hong, J. W. Lee, and W. B. Jeong, "Rheology and Curing of Hydroxyl Terminated Polybutadiene/(Sugar or Calcium Carbonate) Suspension," *Polymer Korea*, vol. 38, no. 4, pp. 417–424, Jul. 2014, doi: 10.7317/pk.2014.38.4.417.
6. H. B. Wibowo, W. C. Dharmawan, and R. S. M. Wibowo, "Bulk Polymerization Kinetics of Hydroxy Terminated Polybutadiene and Toluene Diisocyanate with Infrared Spectroscopy," *Indonesian Journal of Chemistry*, vol. 18, no. 3, p. 552, Aug. 2018, doi: 10.22146/ijc.24807.
7. P. S. Neudorfl, R. A. Back, and A. E. Douglas, "The absorption spectrum of trans-diimide (N2H2) in the vacuum ultraviolet region1," *Can J Chem*, vol. 59, no. 3, pp. 506–517, Feb. 1981, [Online]. Available: www.nrcresearchpress.com
8. N. Joshi, M. N. Romanias, V. Riffault, and F. Thevenet, "Investigating water adsorption onto natural mineral dust particles: Linking DRIFTS experiments and BET theory," *Aeolian Res*, vol. 27, Aug. 2017, doi: 10.1016/j.aeolia.2017.06.001.
9. H. B. Wibowo, "ISOMERISASI POLIMER MELALUI REAKSI SAIN SAYEF UNTUK MENGUBAH KONFIGURASI HTPB (HYDROXYL TERMINATED POLYBUTADIENE) POLYMER ISOMERIZATION BY SAIN SAYEF REACTION TO MODIFY CONFIGURATION OF HTPB (HYDROXYL TERMINATED POLYBUTADIENE)," *Jurnal Teknologi Dirgantara*, vol. 14, no. 2, pp. 137–146, 2016.
10. P. S. Gopala Krishnan, K. Ayyaswamy, and S. K. Nayak, "Hydroxy Terminated Polybutadiene: Chemical Modifications and Applications," *Journal of Macromolecular Science, Part A*, vol. 50, no. 1, pp. 128–138, Jan. 2013, doi: 10.1080/10601325.2013.736275.
11. A. H. Navarchian, F. Picchioni, and L. P. B. M. Janssen, "Rheokinetics and effect of shear rate on the kinetics of linear polyurethane formation," *Polym Eng Sci*, vol. 45, no. 3, pp. 279–287, Mar. 2005, doi: 10.1002/pen.20280.
12. R. Bardestani, G. S. Patience, and S. Kaliaguine, "Experimental methods in chemical engineering: specific surface area and pore size distribution measurements—BET, BJH, and DFT," *Can J Chem Eng*, vol. 97, no. 11, Nov. 2019, doi: 10.1002/cjce.23632.
13. E. Betoret, N. Betoret, J. V. Carbonell, and P. Fito, "Effects of pressure homogenization on particle size and the functional properties of citrus juices," *J Food Eng*, vol. 92, no. 1, pp. 18–23, May 2009, doi: 10.1016/j.jfoodeng.2008.10.028.
14. P. S. Argade, D. D. Magar, and R. B. Saudagar, "Solid Dispersion: Solubility Enhancement Technique for poorly water soluble Drugs," *Journal of Advanced Pharmacy Education & Research*, vol. 3, no. 4, pp. 427–439, 2013, [Online]. Available: www.japer.in

15. A. Kornilov and I. Safonov, "An Overview of Watershed Algorithm Implementations in Open Source Libraries," *J Imaging*, vol. 4, no. 10, Oct. 2018, doi: 10.3390/jimaging4100123.
16. J. K. Chen and T. B. Brill, "Chemistry and kinetics of hydroxyl-terminated polybutadiene (HTPB) and diisocyanate-HTPB polymers during slow decomposition and combustion-like conditions," *Combust Flame*, vol. 87, no. 3–4, pp. 217–232, Dec. 1991, doi: 10.1016/0010-2180(91)90109-O.
17. J. Guo *et al.*, "Kinetic Research on the Curing Reaction of Hydroxyl-Terminated Polybutadiene Based Polyurethane Binder System via FT-IR Measurements," *Coatings*, vol. 8, no. 5, p. 175, May 2018, doi: 10.3390/coatings8050175.
18. H. B. Wibowo, "Current solid propellant research and development in Indonesia and its future direction," *J Phys Conf Ser*, vol. 1130, Nov. 2018, doi: 10.1088/1742-6596/1130/1/012027.
19. V. E. Bondybey and J. W. Nibler, "Infrared and Raman spectra of solid and matrix isolated diimide, HNNH," *J Chem Phys*, vol. 58, no. 5, pp. 2125–2134, 1973, doi: 10.1063/1.1679478.
20. G. M. Tow and E. J. Maginn, "Cross-Linking Methodology for Fully Atomistic Models of Hydroxyl-Terminated Polybutadiene and Determination of Mechanical Properties," *Macromolecules*, vol. 54, no. 10, pp. 4488–4496, May 2021, doi: 10.1021/acs.macromol.1c00228.
21. G. A. Buchner, M. Rudolph, J. Norwig, V. Marker, C. Gürtler, and R. Schomäcker, "Kinetic Investigation of Polyurethane Rubber Formation from CO_2-Containing Polyols," *Chemie Ingenieur Technik*, vol. 92, no. 3, pp. 199–208, Mar. 2020, doi: 10.1002/cite.201900103.
22. Z. Sun, G. Xi, and X. Chen, "A numerical study of stir mixing of liquids with particle method," *Chem Eng Sci*, vol. 64, no. 2, pp. 341–350, Jan. 2009, doi: 10.1016/j.ces.2008.10.034.
23. V. W. A. Verhoeven, A. D. Padsalgikar, K. J. Ganzeveld, and L. P. B. M. Janssen, "A kinetic investigation of polyurethane polymerization for reactive extrusion purposes," *J Appl Polym Sci*, vol. 101, no. 1, pp. 370–382, Jul. 2006, doi: 10.1002/app.23848.
24. M. J. Zdilla, S. A. Hatfield, K. A. McLean, L. M. Cyrus, J. M. Laslo, and H. W. Lambert, "Circularity, Solidity, Axes of a Best Fit Ellipse, Aspect Ratio, and Roundness of the Foramen Ovale," *Journal of Craniofacial Surgery*, vol. 27, no. 1, pp. 222–228, Jan. 2016, doi: 10.1097/SCS.0000000000002285.
25. W. Du, L. Tan, Y. Zhang, H. Yang, and H. Chen, "Rheological and kinetic investigation into isothermal curing of a thermoset polythiourethane system," *Polymer-Plastics Technology and Materials*, vol. 59, no. 1, pp. 63–71, Jan. 2020, doi: 10.1080/25740881.2019.1625381.
26. A. Tanver, M. H. Huang, Y. J. Luo, and Z. H. Hei, "Chemical Kinetic Studies on Polyurethane Formation of GAP and HTPB with IPDI by Using In Situ FT-IR Spectroscopy," *Adv Mat Res*, vol. 1061–1062, pp. 337–341, Dec. 2014, doi: 10.4028/www.scientific.net/AMR.1061-1062.337.
27. L. Sun, Z. Zong, W. Xue, and Z. Zeng, "Mechanism and kinetics of moisture-curing process of reactive hot melt polyurethane adhesive," *Chemical Engineering Journal Advances*, vol. 4, p. 100051, Dec. 2020, doi: 10.1016/j.ceja.2020.100051.
28. F. S. Toosi, M. Shahidzadeh, and B. Ramezanzadeh, "An investigation of the effects of pre-polymer functionality on the curing behavior and mechanical properties of HTPB-based polyurethane," *Journal of Industrial and Engineering Chemistry*, vol. 24, pp. 166–173, Apr. 2015, doi: 10.1016/j.jiec.2014.09.025.
29. B. Lucio and J. L. de la Fuente, "Rheological cure characterization of an advanced functional polyurethane," *Thermochim Acta*, vol. 596, pp. 6–13, Nov. 2014, doi: 10.1016/j.tca.2014.09.012.
30. T. Chai *et al.*, "Rheokinetic analysis on the curing process of HTPB-DOA- MDI binder system," *IOP Conf Ser Mater Sci Eng*, vol. 137, p. 012069, Jul. 2016, doi: 10.1088/1757-899X/137/1/012069.
31. B. Lucio and J. L. de la Fuente, "Kinetic and thermodynamic analysis of the polymerization of polyurethanes by a rheological method," *Thermochim Acta*, vol. 625, pp. 28–35, Feb. 2016, doi: 10.1016/j.tca.2015.12.012.
32. G. Santhosh, S. Reshmi, and C. P. Reghunadhan Nair, "Rheokinetic characterization of polyurethane formation in a highly filled composite solid propellant," *J Therm Anal Calorim*, vol. 140, no. 1, pp. 213–223, Apr. 2020, doi: 10.1007/s10973-019-08793-6.
33. Y. Ou, Y. Sun, and Q. Jiao, "Properties related to linear and branched network structure of hydroxyl terminated polybutadiene," *e-Polymers*, vol. 18, no. 3, pp. 267–274, May 2018, doi: 10.1515/epoly-2017-0223.
34. R. Kumar, A. Singh, M. Kumar, P. K. Soni, and V. Singh, "Investigations of effect of hydroxyl-terminated polybutadiene-based polyurethane binders containing various curatives on thermal decomposition behaviour and kinetics of energetic composites," *J Therm Anal Calorim*, vol. 145, no. 5, pp. 2417–2430, Sep. 2021, doi: 10.1007/s10973-020-09773-x.

35. M. Hui *et al.*, "Kinetic studies on the cure reaction of hydroxyl-terminated polybutadiene based polyurethane with variable catalysts by differential scanning calorimetry," *e-Polymers*, vol. 17, no. 1, pp. 89–94, Jan. 2017, doi: 10.1515/epoly-2016-0245.
36. S. Lee, C. H. Choi, I.-K. Hong, and J. W. Lee, "Polyurethane curing kinetics for polymer bonded explosives: HTPB/IPDI binder," *Korean Journal of Chemical Engineering*, vol. 32, no. 8, pp. 1701–1706, Aug. 2015, doi: 10.1007/s11814-014-0366-y.
37. S. Lee, J. H. Choi, I.-K. Hong, and J. W. Lee, "Curing behavior of polyurethane as a binder for polymer-bonded explosives," *Journal of Industrial and Engineering Chemistry*, vol. 21, pp. 980–985, Jan. 2015, doi: 10.1016/j.jiec.2014.05.004.
38. X. Song and Y. Luo, "Curing kinetics study on interpenetrating polymer networks based on modified hyperbranched polyether/polyurethane," *Monatshefte für Chemie - Chemical Monthly*, vol. 148, no. 7, pp. 1323–1328, Jul. 2017, doi: 10.1007/s00706-017-1987-8.
39. X. Song and L. Yunjun, "Effect of hyperbranched polyesters on HTPB polyurethane curing kinetic," *Materials Research*, vol. 17, no. 1, pp. 78–82, Dec. 2013, doi: 10.1590/S1516-14392013005000193.